Medical Engineering & Physics 34 (2012) 437–446

Contents lists available at ScienceDirect

Medical Engineering & Physics

journal homepage: www.elsevier.com/locate/medengphy

A nonparametric feature for neonatal EEG seizure detection based on a representation of pseudo-periodicity☆

N.J. Stevenson[a,*], J.M. O'Toole[b], L.J. Rankine[a], G.B. Boylan[a], B. Boashash[c,e]

[a] Neonatal Brain Research Group, University College Cork, Cork, Ireland
[b] DeustoTech, University of Deusto, Bilbao, Spain
[c] College of Engineering, Qatar University, Qatar
[d] Future Assist Financial Services, Gold Coast, Australia
[e] University of Queensland Centre for Clinical Research, Brisbane, Australia

ARTICLE INFO

Article history:
Received 25 November 2010
Received in revised form 23 June 2011
Accepted 9 August 2011

Keywords:
Neonatal EEG
Fourier transform
Time-frequency distributions
Nonstationary
Matched filter
Neonate
Seizure detection
Time-frequency signal processing

ABSTRACT

Automated methods of neonatal EEG seizure detection attempt to highlight the evolving, stereotypical, pseudo-periodic, nature of EEG seizure while rejecting the nonstationary, modulated, coloured stochastic background in the presence of various EEG artefacts. An important aspect of neonatal seizure detection is, therefore, the accurate representation and detection of pseudo-periodicity in the neonatal EEG. This paper describes a method of detecting pseudo-periodic components associated with neonatal EEG seizure based on a novel signal representation; the nonstationary frequency marginal (NFM). The NFM can be considered as an alternative time-frequency distribution (TFD) frequency marginal. This method integrates the TFD along data-dependent, time-frequency paths that are automatically extracted from the TFD using an edge linking procedure and has the advantage of reducing the dimension of a TFD. The reduction in dimension simplifies the process of estimating a decision statistic designed for the detection of the pseudo-periodicity associated with neonatal EEG seizure. The use of the NFM resulted in a significant detection improvement compared to existing stationary and nonstationary methods. The decision statistic estimated using the NFM was then combined with a measurement of EEG amplitude and nominal pre- and post-processing stages to form a seizure detection algorithm. This algorithm was tested on a neonatal EEG database of 18 neonates, 826 h in length with 1389 seizures, and achieved comparable performance to existing second generation algorithms (a median receiver operating characteristic area of 0.902; IQR 0.835–0.943 across 18 neonates).

1. Introduction

The accurate representation of periodicity is an important requirement in biological signal processing applications. The aim of such methods is to provide a compact representation in the frequency domain that is more conducive to simpler processing and effective decision making. The need to quantify this repetition has resulted in the widespread use of the magnitude squared of a Fourier transform referred to in this paper as the Fourier spectrum (FS) [1]. The advantage of the FS is that a periodic signal is compactly represented by a peak located at the frequency of repetition.

The ability of the FS to compactly represent periodicity has been exploited for the detection of seizure in neonatal EEG [2,3]. Neonatal seizure detection has become an important problem in neonatal neurology as recent research has shown that seizures damage the developing brain [4–6]. This means that the detection of seizures is useful for diagnosis, leading to treatment, and estimation of the seizure burden (the accumulated duration of seizure) is useful for prognosis [7].

Neonatal EEG seizure, however, is a nonstationary signal which contains stereotypical waveforms that repeat with non-constant period (pseudo-periodicity) [8]. This nonstationarity reduces the ability of Fourier-based methods to compactly represent such signals as they tend to spread the power of these signals over the range of the frequency variation in the signal. This means that it is difficult to associate pseudo-periodicity with an observed peak in the frequency domain. The inability of the FS to represent pseudo-periodicity is apparent in automated methods of detecting the repetitive aspect of neonatal EEG seizure [2,9,10]. The aim of such automated analyses is to distinguish periods of seizure, defined as *a clear ictal event characterised by the appearance of sudden, repetitive, evolving, stereotyped waveforms that have a definite beginning, middle and end, and last for a minimum of 10 s*, from neonatal EEG background or nonseizure which is defined as a disorganised signal with

☆ The Matlab code for the NFM is available at http://www.ucc.ie/en/neonatalbrain/.

* Corresponding author. Tel.: +353 21 420 5940.
E-mail address: n.stevenson@ucc.ie (N.J. Stevenson).

1350-4533/$ – see front matter © 2011 IPEM. Published by Elsevier Ltd. All rights reserved.
doi:10.1016/j.medengphy.2011.08.001

mixed frequency content [11]. These definitions have resulted in the neonatal EEG seizure signal being modelled as a nonstationary multicomponent signal and neonatal EEG background being modelled as a coloured stochastic process [12,13]. An important prerequisite of neonatal EEG seizure detection is, therefore, the accurate representation and detection of repetitive behaviour in the neonatal EEG; a behaviour which has been related to the presence of nonstationary signal components. Once repetition has been identified then the EEG signal must be analysed for amplitude evolution and stereotypical behaviour to accurately determine the presence of seizure. This additional analysis must be undertaken as EEG artifacts, generated by electrical mains interference, ECG, respiration, ocular movements and handling of the neonate, may exhibit periodicity [14]. Accurate methods for detecting nonstationary signal components in neonatal EEG constitutes further refinement to automated neonatal seizure detection methods.

There are many methods that can be applied to the task of detecting nonstationary signal components such as the Radon transform [15], the marginal of a unitary transformed time-frequency distribution (TFD) [16], time-frequency (TF) template matching [17] and data-driven searching of a TFD [18]. These methods, essentially, integrate a TFD along a series of TF paths to form the detector output. The Radon transform uses a series of linear paths with different offsets. The marginal of a unitary transformed TFD overcomes the limitation of linearity by permitting nonlinear functions, but only a single nonlinear function can be selected. This limitation is overcome by using a TF template matching procedure in which several templates that highly correlate with the TF representation of seizure can be selected. The weakness of the TF template matching procedure is that a restriction on the number of templates must be enforced to minimise both the computational burden and the false alarm rate. This results in a reduction in detector performance as not all seizure patterns are accounted for by the template set. The need for *a priori* information to form an optimal, reduced template set is overcome by using data-driven TF paths estimated from the TFD [18]. The detector output is then generated by correlating frequency shifted versions of this TF path with the signal. The limitation of this method is that only a single optimal TF path is generated which results in reduced detection performance when signals with multiple signal components, such as neonatal EEG seizure, are considered. This paper aims to enhance the technique of [18] to include multiple signal components and apply this method to the estimation of a decision statistic designed for the detection of pseudo-periodic components associated with neonatal EEG seizure.

This paper first outlines the application of a nonstationary model of the neonatal EEG signal to the problem of seizure detection. The relationship between detecting nonstationary signal components and neonatal EEG seizure is defined and a simple decision statistic is proposed based on the model. The basis of a nonstationary signal component detector, the nonstationary frequency marginal (NFM), is then introduced as an alternative method of constructing a data-dependent frequency marginal of a TFD that accounts for the nonstationary characteristics of a signal. Relevant information on TFDs including the marginal satisfaction condition of TFDs that links a TFD to the FS (the basis of an optimal detector for stationary signal components) is presented. The ability of the NFM to improve the detection of pseudo-periodic signal components was tested and the results were compared with a FS based detector and other nonstationary methods, such as TF template matching and TF Rényi entropy [17,19]. The decision statistic was then combined with a measurement of EEG amplitude (an approximation to the amplitude-integrated EEG [20]) in a trained linear discriminant classifier (LDC), with pre- and post-processing stages, to form a seizure detection algorithm (SDA). The performance of the SDA was analysed using a leave-one-subject-out cross-validation [21].

2. Method

2.1. Neonatal EEG acquisition

The data used throughout this paper were acquired at the Cork University Maternity Hospital, Ireland. The EEG recordings were acquired with a multiple channel video-EEG (NicoletOne, CareFusion, San Diego, USA). The recording electrodes of the EEG were positioned according to the international 10–20 system, modified for neonates [14]. The initial data set contained 826 h of data, recorded from 18 neonates. All data were sampled at 256 Hz after analogue filtering with a pass band of [0.5, 70] Hz to prevent baseline drift and aliasing. Two experienced neurophysiologists used an 8-channel bipolar montage to, independently, determine the presence of seizures in the recording. There were 1389 seizures identified in this database with a mean duration of 194 s and a median duration of 93 s; of these 898 were greater than 64 s in duration (median 166 s) and 491 were less than or equal to 64 s in duration (median 38 s). The seizure burden (median 162 min, IQR 101–239 min), mean seizure duration (median 249 s, IQR 96–356 s), recording length (median 50.6 h, IQR 29.7–59.8 h) and the artefact burden (median 4.9 h, IQR 3.8–5.4 h) were recorded for each neonate. The ratio of seizure to nonseizure duration (median 5.9%, IQR 4.2–12.1%) was also recorded. The EEG data were down-sampled to 8 Hz to decrease the computational burden of the NFM. The down-sampling procedure used digital anti-aliasing filters.

A sub-sample of the database of neonatal EEG was used to develop the NFM-based feature. This database was constructed by randomly selecting one hundred 64 s epochs from seizure events lasting more than 64 s, one hundred 64 s epochs from seizure events lasting less than 64 s, and two hundred 64 s epochs from the remaining artefact-free background EEG (only low frequency EEG seizures (<4 Hz) were included in the sub-sampled data set). All physiological recordings were performed according to the ethics of the University College Cork and the Cork University Maternity Hospital. Example epochs of EEG seizure and background are shown in Fig. 1.

2.2. A nonstationary model for neonatal EEG seizure detection

A simple model of neonatal EEG can be defined as,

$$\mathrm{EEG}(t) = k_s(t)\mathrm{seizure}(t) + k_b(t)\mathrm{background}(t). \quad (1)$$

where seizure(t) and, background(t), are assumed to have equal signal energy. The time-varying gain, $k_s(t)$, is used to effectively turn seizure on and off and time-varying gain, $k_b(t)$, is used to simulate longer term modulations of the background such as seen in active and quiet sleep [13].

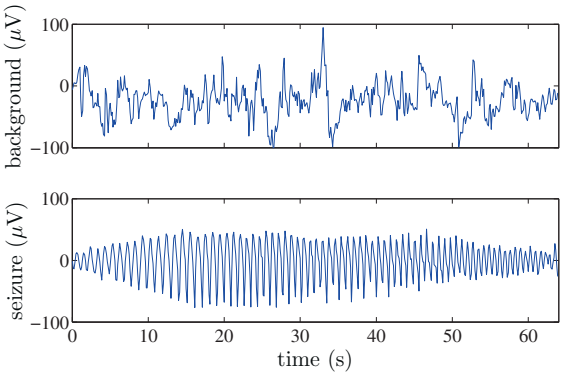

Fig. 1. Example 64 s epochs of neonatal EEG seizure and background.

The seizure signal has been modelled in [12]. The analytic associate of this signal model [22, p. 86] is defined as,

$$\text{seizure}(t) = \sum_{i=1}^{R} a_i(t) \exp\left(j2\pi \int_0^t f_i(\tau)\, d\tau + \phi_i\right), \tag{2}$$

where $a_i(t)\exp\left(j2\pi \int_0^t f_i(\tau)\, d\tau + \phi_i\right)$ is the ith nonstationary signal component and R is the number of components. The use of the product of two functions in the definition means that there can be a large number of choices of $a_i(t)$ and $f_i(t)$ that result in seizure(t). A practically useful definition of $a_i(t)$ and $f_i(t)$ can be obtained by ensuring the frequency content of the AM is significantly less than the IF [23,24]. This restriction permits the interpretation of these functions as the amplitude modulation (AM) and the frequency modulation (FM) (or instantaneous frequency (IF)), respectively. The IF of each signal component characterises the pseudo-periodicity in the signal [17]. The application of this model to neonatal EEG seizure results in the additional constraints of a harmonic relationship between components ($f_i = if_1$) and a minimum component duration of 10 s [11].

The background function has been modelled as [25],

$$\text{background}(t) = \text{IFT}\left\{\frac{X(f)}{f^{(2H+1)}}\right\}, \tag{3}$$

where IFT is the inverse Fourier transform, $X(f)$ is the spectrum of a single realisation of white noise and H is the Hurst exponent of a fractional Brownian process which is limited between 0 and 1 [25]. This process is further filtered by a bandpass filter simulating data acquisition.

A power based decision statistic can be proposed by incorporating the fact that neonatal EEG is segmented into epochs and assuming that a decision is made per epoch. The power ratio decision statistic is defined as,

$$\eta(u) = \frac{\left|\int_{u-T/2}^{u+T/2} k_s(t)\text{seizure}(t)\, dt\right|^2}{\left|\int_{u-T/2}^{u+T/2} k_b(t)\text{background}(t)\, dt\right|^2}, \tag{4}$$

where the integration of the uth epoch is performed for duration T. If this value is greater than some threshold then seizure is present and if less than or equal to some threshold then background is present. An approximation to the decision statistic on the complex version of the EEG is defined as,

$$\eta(u) \approx \frac{\int_{u-T/2}^{u+T/2} \sum_{i=1}^{R} |k_s(t)a_i(t)|^2\, dt}{\int_{u-T/2}^{u+T/2} |k_b(t)|^2\, dt}, \tag{5}$$

where $k_s(t)a_i(t)$ and $k_b(t)$ are real. This approximation utilises Schwartz's inequality [26, p. 449]. If the frequency of the seizure is constant, η is closely related to the spectral power ratio used in the neonatal seizure detection algorithm outlined by Gotman et al. [2]. In order to estimate $\eta(u)$, significant, harmonically related, nonstationary signal components must, therefore, be detected in the neonatal EEG.

A method of nonstationary signal component detection can be developed by extending the method of optimal detection for stationary signal components to deal with nonstationary signal components. For stationary signal components, an optimal detector can be constructed from a peak detector applied to the FS. The performance of this detector is reduced when detecting nonstationary signal components due to the smearing of energy in the frequency domain. A peak detector applied to a signal representation similar to the FS that does not smear energy in the frequency domain in the presence of nonstationary signal components (Fig. 2(c) and (d)) would result in near optimal detection. The NFM is a novel representation that can super resolve the nonstationary signal components seen in neonatal EEG seizure.

2.3. Nonstationary frequency marginal

The NFM was designed to represent nonstationary signal components on a frequency domain. The formulation of the NFM requires a signal representation that is capable of accurately representing the time-varying frequency content of nonstationary signal components. TFDs were chosen as they represent signal energy on a joint-time frequency domain. The quadratic class of TFDs is defined as [22],

$$\rho_\gamma(t,f) = W_z(t,f) \underset{(t,f)}{**} \gamma(t,f), \tag{6}$$

where $*$ is the convolution operation, and $\gamma(t,f)$ is the filter that characterises different TFDs, such as the spectrogram, separable kernel, or Choi–Williams distribution [22], within the quadratic class. $W_z(t,f)$ is the Wigner–Ville distribution (WVD) which is defined as [22, p. 30],

$$W_z(t,f) = \int_{-\infty}^{\infty} z\left(t+\frac{\tau}{2}\right) z^\star\left(t-\frac{\tau}{2}\right) e^{-j2\pi f\tau}\, d\tau, \tag{7}$$

where $z(t)$ is the analytic associate of the real signal under analysis, that is, $z(t) = s(t) + j\mathcal{H}\{s(t)\}$ where $\mathcal{H}$ is the Hilbert transform, $z^\star(t)$ denotes the complex conjugate of $z(t)$, f is frequency, t is time and τ is time lag.

An important property of the WVD is the satisfaction of the marginal conditions [22, p. 60], that is,

$$|z(t)|^2 = \int_{-\infty}^{\infty} W_z(t,f)\, df \quad \text{and} \tag{8}$$

$$|Z(f)|^2 = \int_{-\infty}^{\infty} W_z(t,f)\, dt, \tag{9}$$

where $|Z(f)|^2$ is related to the FS ($|S(f)|^2$) of the real signal, $s(t)$, via [22, p. 13],

$$|Z(f)|^2 = \begin{cases} 4|S(f)|^2, & f > 0 \\ |S(f)|^2, & f = 0 \\ 0, & f < 0 \end{cases}. \tag{10}$$

The WVD, in the presence of multicomponent signals, is affected by interference generated by the quadratic nature of the transformation. As the interference tends to be highly oscillatory a simple method of reducing it, is to filter or smooth the WVD with a 2D lowpass filter [22]. The smoothness of a TFD can be improved by increasing the effective bandwidth duration (BT) product of the smoothing filter [23].

The NFM identifies signal components in a TFD of the signal under analysis and then integrates the TFD along the TF paths of the identified components. The resultant energy of integration is then located at the mean TF path frequency to generate an alternate signal representation. The process of generating a signal representation by integrating along data-dependent TF paths, as opposed to generating a normal frequency marginal (9) results in improved detection of nonstationary signal components. The formulation of the NFM as a data-dependent integration of a TFD and the alternate signal representation it generates are shown in Fig. 2.

The NFM identifies TF paths using the multiple component IF estimation technique outlined in [27]. This method converts a TFD

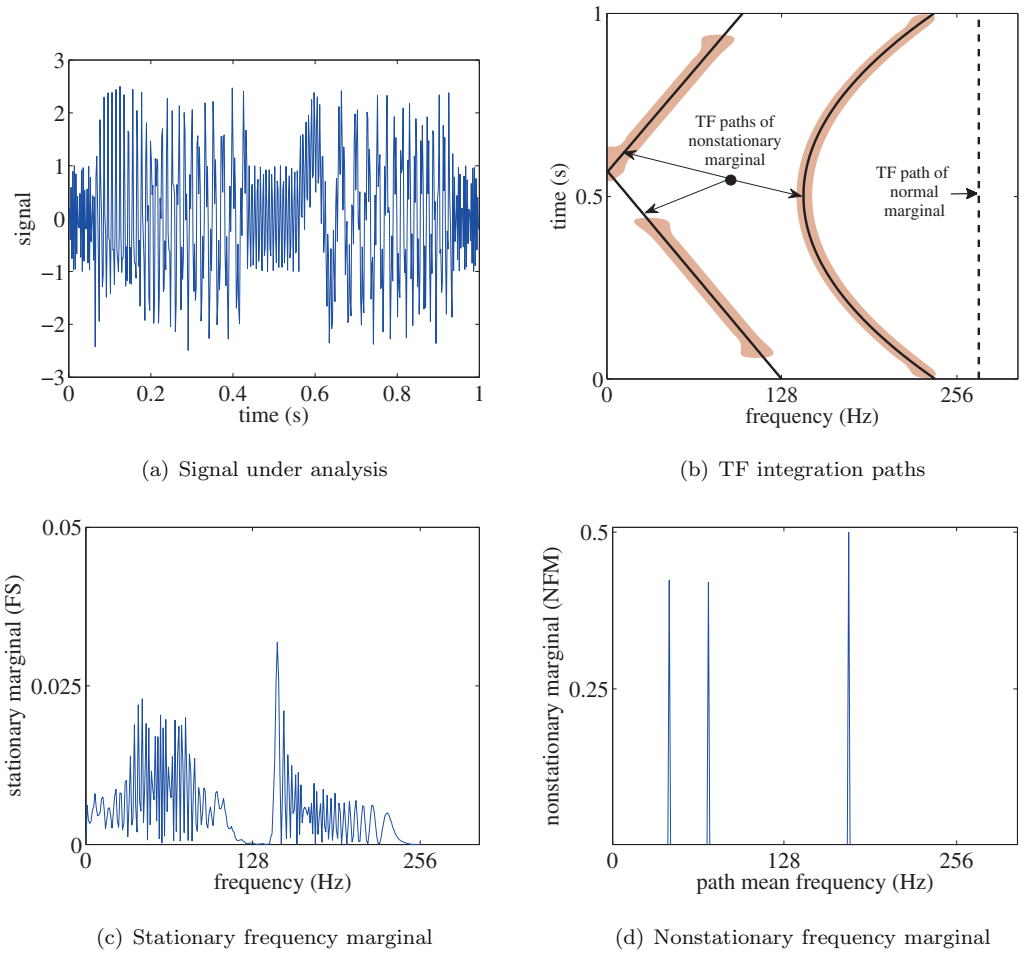

(a) Signal under analysis

(b) TF integration paths

(c) Stationary frequency marginal

(d) Nonstationary frequency marginal

Fig. 2. Data-dependent integration of a TFD. The signal under analysis is shown in (a), the TFD of the signal and the TF paths used to integrate the TFD for the NFM and FS are shown in (b), the FS of the signal is shown in (c) and the NFM is shown in (d). The shaded region in (b) denotes the concentration of signal energy in the joint TF plane (the TF representation was a WVD smoothed with a separable kernel – 2D Hanning window) and the energy between (c) and (d) is conserved. The peaks in (d) correspond to signal components with mean frequencies of [43, 72, 176] Hz and powers of [0.42, 0.42, 0.5], respectively.

to a binary image, in which one denotes the presence of local maxima and zero the absence of any maxima, that is,

$$b(n,m) = \begin{cases} 1 & \text{if } \dfrac{\partial \rho_\gamma(n,m)}{\partial m} \geq 0 \text{ and } \dfrac{\partial \rho_\gamma(n,m+1)}{\partial m} < 0 \\ 0 & \text{otherwise} \end{cases}, \qquad (11)$$

where $b(n,m)$ is the binary image, $\rho_\gamma(n,m)$ is the discrete TFD of discrete signal $s(n)$, n and m are discrete time and discrete frequency respectively. The partial derivatives are found using a forward difference approximation [28, p. 106]. The work reported in [27] ignores the low energy regions of the TFD, but the NFM considers the entire region of the TFD.

This binary image is then searched for maxima that are located within a pre-defined search area using an edge linking algorithm [29]. Maxima that are located within the search area are linked together to form a single TF path. Example search areas are shown in Fig. 3(a) for marginal satisfaction (a search that generates the FS) and Fig. 3(b) an alternate representation of nonstationary signal components (a search that generates the NFM). The extent of the search area is typically related to the amount of smoothing in the TFD and the only restriction is that the current row along the frequency axis is not included. This restriction is based on the fact that two maxima cannot occur on consecutive discrete frequency samples, due to (11), and the assumption that maxima occurring further away are associated with separate TF paths. This also ensures a one-to-one relationship between time and frequency which conserves the continuity of the TF path with respect to time. The edge linking procedure also permits a lower limit on the length of components to be identified.

The edge linking algorithm extracts R paths with lengths, $\mathbf{L} = [L_1, L_2, L_3, \ldots, L_R]$, that are defined by time vector $\mathbf{p} = [p_1, p_2, p_3, \ldots, p_R]$, and frequency vector $\mathbf{q} = [q_1, q_2, q_3, \ldots, q_R]$, where the discrete IF of the ith TF path is one-to-one and defined as $q_i(p_i)$. The TFD is then integrated along these TF paths and the result is assigned to the mean frequency of the ith TF path ($\bar{m}_i$) to provide information on the frequency content of the nonstationary signal component. The mean frequency domain, m_p (a dummy frequency variable), is sampled identically to the frequency domain of the normal frequency marginal ($m_p \equiv m$). The residual TFD energy, not represented by a TF path, is then added to the energy associated with the TF paths to conserve overall signal energy. This NFM is, therefore, defined with respect to discrete path mean frequency, m_p, as

$$\mathrm{NFM}(m_p) = \left(\sum_{i=1}^{R} \mathrm{ms}_i(m_p) \right) + \mathrm{residual}(m_p), \qquad (12)$$

where

$$\mathrm{ms}_i(m_p) = \delta(m_p - \bar{m}_i) \sum_{k=1}^{L_i} \rho_\gamma\left(p_i(k), q_i(k)\right), \qquad (13)$$

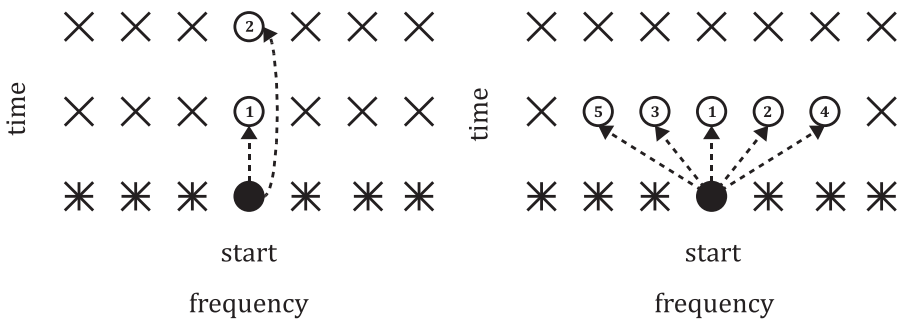

(a) Search for marginal satisfaction (b) Default search

Fig. 3. Search regions for the edge linking algorithm. The crosses denote possible search locations, circles denote valid search directions, the number in each circle denotes the order of the search and the stars denote invalid search locations.

$\delta(m_p - \bar{m}_i)$ is the delta function defined as,

$$\delta(m_p - \bar{m}_i) = \begin{cases} 1 & m_p = \bar{m}_i \\ 0 & \text{otherwise} \end{cases}, \tag{14}$$

$\bar{m}_i$ is the mean frequency of the path defined as [22],

$$\bar{m}_i = \frac{\sum_{k=1}^{L_i} q_i(k)\rho_\gamma(p_i(k), q_i(k))}{\sum_{k=1}^{L_i} \rho_\gamma(p_i(k), q_i(k))}, \tag{15}$$

$$\text{residual}(m) = \sum_{n=0}^{N-1} \rho_r(n, m), \tag{16}$$

where

$$\rho_r(n, m) = \begin{cases} \rho_\gamma(n, m) & \text{for } n \notin \mathbf{p}, m \notin \mathbf{q} \\ 0 & \text{for } n \in \mathbf{p}, m \in \mathbf{q} \end{cases} \tag{17}$$

and N is the discrete signal length.

The parameters that define the performance of the NFM are: $\gamma(t, f)$ which characterises the TFD, the size and shape of the search region and the minimum path length. Example parameters for a NFM formed using the WVD ($\gamma(t, f) = \delta(t, f)$) are the search region shown in Fig. 3(b) and a minimum path length of 3 samples.

A smoother TFD will generate fewer, longer duration paths which will result in a more discontinuous NFM as more energy will be integrated over fewer paths. The shape of the smoothing window, the design of the search region and the minimum path length can be used to emphasise a particular signal class in the NFM. If for example, long duration signal components with slowly varying IF laws, such as neonatal EEG seizure, are to be represented, then the NFM should be implemented using a TFD with a low bandwidth/long duration smoothing window and search region and, a long minimum path duration [30]. The ratio of bandwidth to duration can easily be controlled using a separable kernel [22].

The use of smoothed WVDs permits some modification to the implementation of the NFM. The TF paths used to form the NFM are widened to the −3 dB bandwidth (BW_3) of the smoothing window to take into account the spreading of energy in the TFD due to the smoothing process. The search area is also widened by BW_3. Finally, the minimum path length is extended to $2BW_3$.

3. Results

The NFM was applied to the task of detecting pseudo-periodic components associated with neonatal EEG seizure. The neonatal EEG was pre-whitened (via a differentiator), as recommended in [9,13]. An estimate of the test statistic in (5) was used as a basis for the detector. The practical, automated implementation of (5) resulted in a definition of η per epoch of neonatal EEG as

$$\eta \approx \frac{\sum_{n=1}^{\lfloor M/m_h \rfloor} S(m_h n)}{\left(\sum_{m=0}^{M-1} S(m)\right) - \sum_{n=1}^{\lfloor M/m_h \rfloor} S(m_h n)}, \quad m = [0, \ldots M-1], \tag{18}$$

where $m_h = \text{argmax}(S(m))$, m is discrete path frequency or frequency, M is the discrete length of $S(m)$, and $S(m)$ the representation under trial (e.g. the FS or NFM). Due to possible bias in the estimation of the path mean frequency, a 10% error margin is searched to find the peak harmonic of any harmonics.

The estimate of the background power, represented in the denominator, is equivalent to that in (5) if the background and seizure waveforms are assumed to be orthogonal (or near orthogonal) to each other. Orthogonality ensures that the combined power in the seizure and background components is the equivalent of the power in the combined EEG signal. This is a reasonable assumption if the pre-whitened background is a white noise process [26].

The NFM was estimated from a TFD smoothed with a separable kernel; a two-dimensional Hanning window (−3 dB duration of 2.125 s, −3 dB bandwidth of 0.133 Hz). The shape of the 2D Hanning window improves the detection of slowly varying pseudo-periodic components seen in neonatal EEG seizure [30]. The minimum component length was set to 10 s as defined in [11].

The discriminatory ability of η, estimated with both the NFM and FS, was tested against a small database of artefact-free EEG over a range of epoch lengths. The performance of η was quantified using a receiver operator characteristic (ROC). The ROC was constructed by plotting the sensitivity against the specificity as the threshold was varied from the minimum to maximum value of η. The sensitivity was defined as the number of seizure epochs correctly identified and the specificity was defined as the number of background epochs correctly identified, in percentages. The area under the ROC (AUC) and the point at which the ROC crosses the line of equal sensitivity and specificity were reported. This feature was then tested on a large database of neonatal EEG, collected as part of normal monitoring of the neonate (inclusive of artefact). Its performance was compared to a measurement of aEEG amplitude which has shown to provide important information for the detection of seizure [3]. Finally, the NFM based estimate of η was combined with aEEG amplitude using a trained LDC, with pre-processing and post-processing stages, to form a simple SDA. This SDA was tested on the full database of neonatal EEG and assessed with the AUC, seizure

Table 1
Detecting short and long duration events with pseudo-periodicity (seizure) in neonatal EEG over a range of analysis window durations. The results are presented as mean above (standard deviation). The percentage value is the point at which sensitivity equals specificity on the ROC. Values in bold are associated with the maximum AUC.

Epoch length (s)	8	16	32	64
Seizure events >64 s				
η (FS)	0.882	0.938	0.835	0.690
	(0.024)	(0.015)	(0.029)	(0.036)
	83.1%	85.4%	78.8%	62.8%
	(2.9)	(2.6)	(2.9)	(3.5)
η ($NFM_{0.3}$)	0.841	0.953	**0.977**[*]	0.965
	(0.028)	(0.015)	(0.009)	(0.013)
	76.9%	90.3%	**92.9%**[*]	92.3%
	(3.1)	(2.1)	(2.0)	(2.1)
Seizure events ≤64 s				
η (FS)	0.695	0.734	0.631	0.568
	(0.035)	(0.035)	(0.040)	(0.040)
	64.2%	67.3%	63.6%	55.9%
	(3.3)	(3.5)	(3.4)	(3.6)
η ($NFM_{0.3}$)	0.790	0.863	0.909	**0.915**[*]
	(0.033)	(0.025)	(0.024)	(0.020)
	73.4%	78.3%	84.7%	**85.3%**
	(3.4)	(3.1)	(2.2)	(2.7)

[*] Statistically significant improvement compared to the best performing FS. (t-test, level of significance 0.05).

Table 2
Comparing different methods of detecting pseudo-periodicity (seizure) in neonatal EEG over a range of analysis window durations. The results are presented as mean (standard deviation). The percentage value in brackets is the point at which sensitivity equals specificity on the ROC. Values in bold are associated with the maximum AUC.

Epoch length (s)	8	16	32	64
η (FS)	0.818	0.855	0.772	0.674
	(0.021)	(0.017)	(0.021)	(0.023)
	73.9%	77.4%	72.2%	64.0%
	(2.2)	(2.0)	(1.9)	(2.4)
η ($NFM_{0.3}$)	0.798	0.903	0.935	**0.944**[*]
	(0.022)	(0.014)	(0.015)	(0.011)
	73.1%	84.1%	86.8%	**88.4%**[*]
	(2.2)	(1.9)	(1.9)	(1.9)
TF-templates	0.923	0.913	0.818	0.649
	(0.013)	(0.014)	(0.022)	(0.031)
	85.7%	83.5%	74.9%	58.1%
	(0.12)	(0.19)	(0.15)	(0.24)
TF Rényi entropy	0.627	0.629	0.714	0.822
	(0.026)	(0.030)	(0.028)	(0.022)
	60.9%	60.7%	66.4%	73.9%
	(2.3)	(2.5)	(2.5)	(2.3)

[*] Statistically significant improvement compared to other methods (t-test, level of significance 0.05).

detection rate and false alarms per hour metrics [31]. Two clinically relevant measures of a SDA are the ability of the SDA to discriminate seizure from nonseizure neonates when applied to long duration EEG recordings and the ability of the SDA to accurately estimate the seizure burden of the neonate. The lack of nonseizure neonates in the test database eliminates the opportunity to estimate the first measure but the accuracy of an estimate of seizure burden at an optimal decision threshold was included.

3.1. Comparison to stationary and nonstationary methods

The FS and the NFM of an 64 s epoch of neonatal EEG seizure and background are shown in Fig. 4. The NFM of neonatal EEG seizure shows power concentrated around 3 TF paths while the distribution of neonatal EEG background power lacks clear structure and is spread over the entire mean frequency domain. The FS is a less compact representation. The difference between the maxima in the FS and NFM with respect to seizure and background suggests a peak detector applied to the NFM would result in greater separation between the pseudo-periodic behaviour of seizure and random behaviour of background.

The test statistic, η, was then estimated using the FS and NFM in order to compare stationary and nonstationary representations. The FS and NFM were additionally estimated using analysis epochs of increasing length to investigate the effect of including more data in the formation of the signal representation. In the case where the analysis epoch was less than 64 s, the original 64 s epoch was divided into overlapping (50% overlap) sub-epochs and the sub-epoch with the maximum feature value was chosen to represent the 64 s epoch. As the minimum duration of a seizure event has been defined as 10 s there may be instances where the seizure duration is significantly less than the duration of the analysis epoch [11]. In order to assess the effect of short duration events, the detector was applied to two subsets of neonatal EEG seizure; the first contains neonatal EEG seizures exceeding 64 s and the second contains neonatal EEG seizures less than 64 s. The results are given in Table 1 where the mean and standard deviation of each performance metric was estimated using a bootstrap with 200 resamplings [32]. Any improvement in the NFM over the FS was tested with Student's t-test and deemed significant if $p < 0.05$.

The test statistic estimated from the FS outperformed the NFM when the analysis epoch was short and the seizures were of long duration, but the FS-based estimate suffered a significant reduction in performance when the duration of the analysis epoch was increased.

The NFM based estimate of η for the detection of seizure was also compared, across various analysis epoch lengths, to other methods based on the detection of pseudo-periodicity: the output of a TFD template matching procedure and the TF Rényi entropy [17,19]. The TFD template matching procedure correlates a limited set of TFD templates with the TFD of the neonatal EEG epoch. The detector output of the TF template matching procedure is,

$$\eta = \max_{(n,m)} \left(\sum_{(r,s)} \rho_\gamma(n,m)\phi_l(n-r,m-s) \right), \quad l = [0,\ldots,L-1], \tag{19}$$

where $\rho_\gamma(n, m)$ is the TFD of the neonatal EEG epoch, $\phi_l(n, m)$ is the lth TF template and L is the number of templates. This is equivalent to a 1D implementation of a matched filter when the TFD satisfies Moyal's equality [33]. This method was developed for seizure detection in the neonate and details can be found in [17]. TF Rényi entropy is commonly used as a measure of signal information content and complexity on the TF domain [19]. A signal that is compactly represented by a TFD, such as neonatal EEG seizure, will have a lower TF Rényi entropy than a signal that is spread in the TF domain such as neonatal EEG background.

The nonstationary methods were implemented on the combined seizure and background neonatal EEG databases (two hundred 64 s epochs of seizure and two hundred 64 s epochs of neonatal EEG background). The results are outlined in Table 2 and the mean and standard deviation of the ROC estimate of each method was calculated using a bootstrap with 200 resamplings. It can be seen that the NFM-based η estimate resulted in the best performance for the detection of the pseudo-periodic component of neonatal EEG seizure and was at a maximum when the epoch length was 64 s.

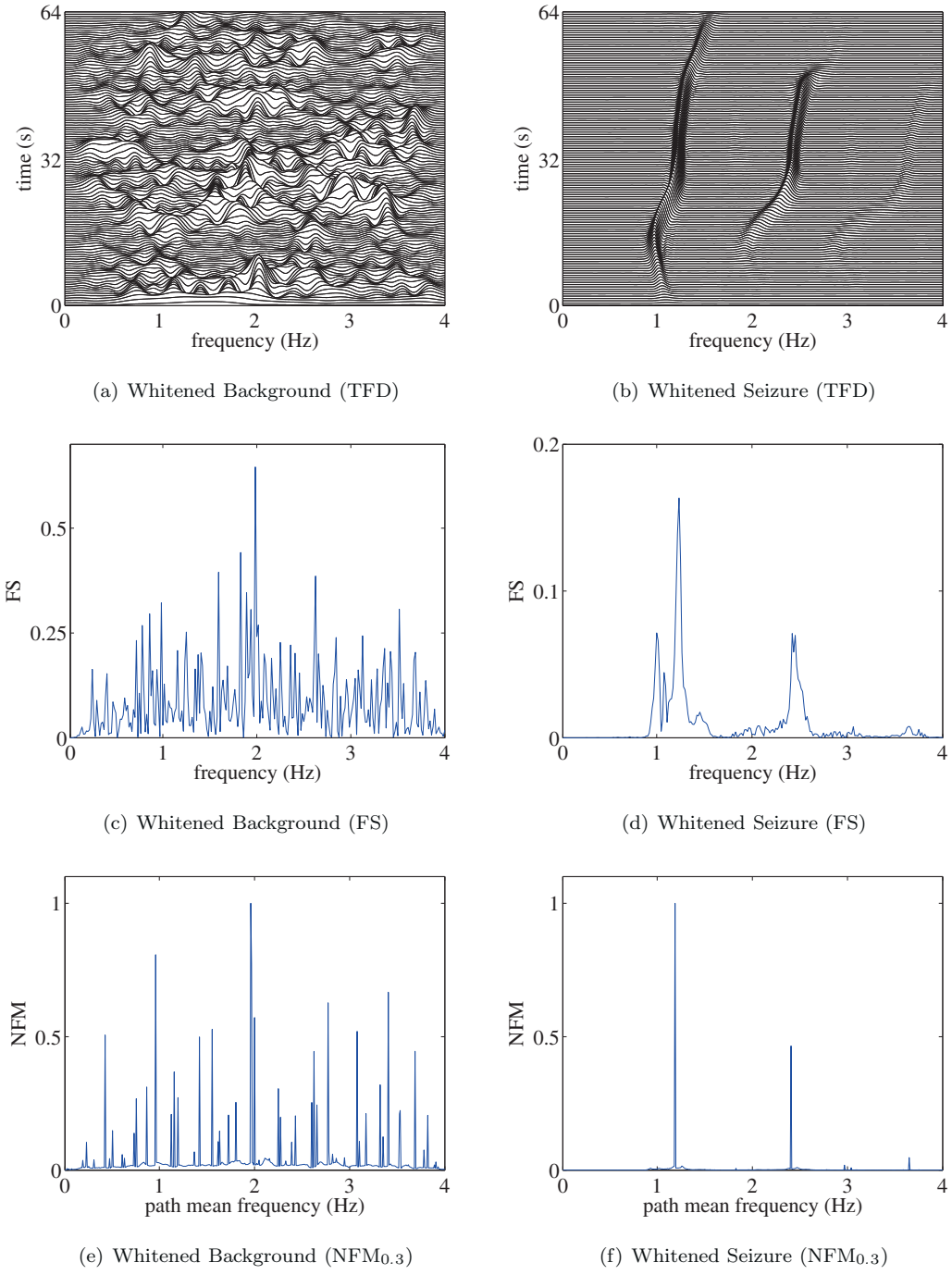

Fig. 4. Representing 64 s epochs of real neonatal EEG (seizure and background), (a) and (d) are the smoothed WVD, (b) and (e) are the FS, and (c) and (f) are the NFM, of real neonatal EEG background and seizure, respectively. The energy between (b) and (c), and (e) and (f), is conserved.

3.2. Performance of η on the full database

The ability of stationary and nonstationary estimates of the decision statistic, η, to discriminate between seizure and non-seizure was then tested on a full database of neonatal EEG. The use of the full database of neonatal EEG exposes each feature to the large array artefacts seen in largely unsupervised long duration recordings of the EEG. Estimates of η, using the NFM and FS, are compared to the aEEG amplitude which has been shown to be a highly discriminatory nonparametric feature for seizure detection [34]. The performance of each feature for detecting seizure from nonseizure is shown in Table 3.

3.3. Neonatal seizure detection

A SDA was developed by combining three features in a LDC and adding pre- and post-processing stages [21]. The features used were

Table 3
The discriminatory performance of η and aEEG amplitude for neonatal seizure detection. The results are presented as median (IQR) across 18 neonates.

	AUC
aEEG amplitude	0.774 (0.697–0.870)
η with NFM	0.849 (0.760–0.870)
η with FS	0.513 (0.451–0.583)

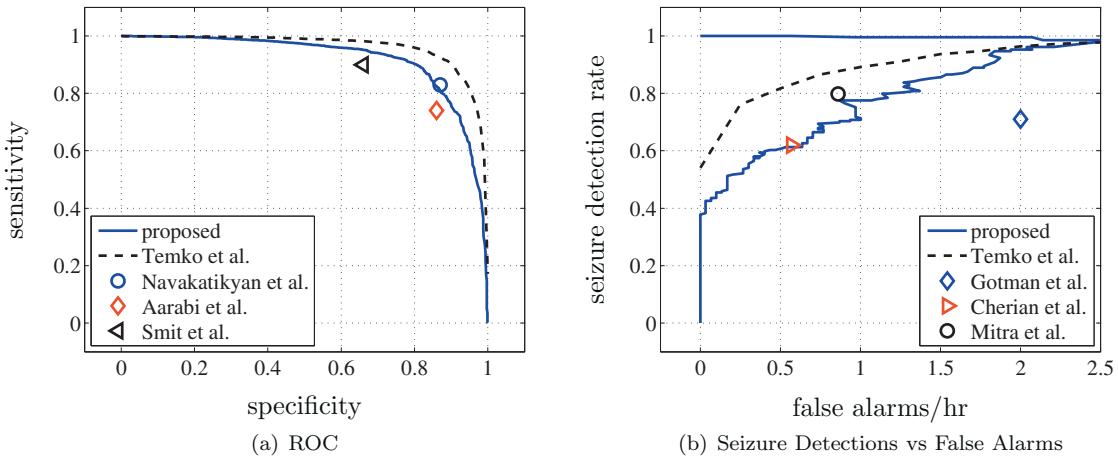

(a) ROC (b) Seizure Detections vs False Alarms

Fig. 5. Performance of the proposed SDA compared to other methods.

Table 4
The differences in SDA performance between low and high performing neonates with respect to and seizure burden, mean seizure duration, recording length and artefact burden.

	Low AUC median (IQR)	High AUC median (IQR)	*p*-Value
Seizure burden (min)	152 (93–252)	183 (89–275)	0.80
Mean seizure duration (s)	303 (96–377)	147 (94–313)	0.44
Seizure number	41 (20–88)	60 (37–163)	0.35
Recording length (h)	48 (28–60)	52 (28–61)	1.00
Artefact burden (%)	13 (7–19)	10 (9–13)	0.67

η, the aEEG and an additional measurement of amplitude, designed to capture information on the long term evolution of the amplitude. This feature is similar in concept to the estimate of background EEG used in [2] and was defined as the lower quartile of the aEEG feature estimated over an hour. The LDC was chosen as the features were developed to be singularly discriminatory so a simple linear division of the feature space should be possible.

The pre-processing stage involved downsampling, segmentation (a 64 s epoch with an overlap of 48 s) and a simple artefact detection system. The artefact detection system eliminated any EEG epoch with an aEEG amplitude greater than 70 μV and a bad electrode annotation (these are automated annotations applied by the EEG machine). The post-processing stage involved taking the maximum classifier output across the 8 EEG channels and smoothing this output with rectangular window 5 epochs in length. A seizure was detected if this smoothed output exceeded a set threshold. A collar of 5 epochs in length was then applied to the detection output.

A leave-one-subject-out cross-validation procedure was used to assess the performance of the SDA [21]. This is an iterative method for estimating the SDA performance on unseen testing data. At each iteration, a training set was formed by leaving out a single subject from the full database. A randomly selected subset of the training set (approximately 10 min of seizure and 100 min of nonseizure per patient) was used to train the LDC which was then tested on the left-out subject. The features were normalised with a Box–Cox transformation [35]. This process was repeated until all subjects had been tested or unseen.

The ROC and the false alarms per hour versus seizure detection rate of the SDA for the median neonate are shown in Fig. 5. The median AUC for the SDA was 0.902 (IQR 0.835–0.943). The reported performance of other SDAs is also shown in Fig. 5[2,3,36,40–44].

The ability of the SDA to provide an accurate measure of the seizure burden was assessed using the absolute error at a single optimal decision threshold. The minimum error in an estimate of seizure burden had a median of 1.92 min/h (IQR 0.45–3.66 min/h) across 18 neonates. The false alarm rate and duration of false alarms at this optimal threshold had a median of 0.11/h (IQR 0.03–0.45/h) and a median of 221 s (IQR, 169–244 s), respectively.

The difference in the highest performing neonates and lowest performing neonates (9 low AUC vs 9 high AUC) with respect to seizure burden, mean seizure duration, recording length and artefact burden were tested using a Mann–Whitney *U* test and the results are summarised in Table 4. Artefact burden was defined as the duration of epochs marked as a bad electrode by the EEG machine or exceeding an aEEG amplitude of 70 μV (equivalent to an average EEG amplitude of 120 μV across the 64 s epoch); therefore it does not contain an estimate of low amplitude artefacts such as those caused by heart rate, respiration, movements, electrical mains interference and electrode pop.

4. Discussion

Accurate detection and measurement of nonstationary signal components results in an improved feature estimate that is important for the detection of seizure in neonatal EEG. The proposed method offers significant improvement over stationary methods and other nonstationary methods for the detection of pseudo-periodicity seen in neonatal EEG seizure. The combination of this feature with measurements of EEG amplitude, pre- and post-processing stages results in a SDA with a performance that is comparable to second generation algorithms.

It is important when forming a spectral estimate that as much data as possible are used to form the estimate; in other words, a long analysis window is required. An increase in the analysis window increases the resolution of the spectral representation of pseudo-periodicity. This is why detection based on the FS is more accurate when using an epoch of 16 s rather than 8 s (Table 2). The assumption in choosing long analysis windows is that signal characteristics do not change within the analysis window, in other words the signal is stationary. In the case of nonstationary signals, such as the neonatal EEG, this assumption is violated and

stationary methods for representing periodicity in a signal suffer a reduction in compactness. This is why detection based on the FS is less accurate as the analysis window length increases above 16 s. In order to overcome nonstationarity in a signal, stationary processing methods must use analysis windows short enough to assume stationarity which results in a reduction in the resolution of a spectral representation and a subsequent reduction in the separability between pseudo-periodic signal components and noise. This led to the development of features based on the information calculated from different estimates of the time-varying autocorrelation function which is fundamental in the definition of TFDs [36,37]. The parametric nature of these features and the heuristic selection of the various thresholds used in their construction suggest that these features are suboptimal, even though the performance of these features for seizure detection is relatively high. It also means their incorporation into an advanced machine learning paradigm is difficult.

The NFM overcomes the constraints of stationary methods by using methods which were designed for nonstationary signals such as TFDs. The NFM compresses a 2D TFD, constructed using a long analysis window, into a 1D signal representation of pseudo-periodicity. This permits the NFM to form a nonparametric representation of pseudo-periodic signal components even if the duration of the pseudo-periodicity is less than the duration of the analysis window. The cost of such an improvement is a more discontinuous representation that is computationally more expensive than the FS due to the use of TFDs (although the NFM can still be implemented in real time as 400, 64 s epochs of neonatal EEG, sampled at 8 Hz, are processed on average in 1.1 s, running on a Intel Core2 Duo E8400 3 GHz in a MATLAB environment). The NFM is also not invertible, like the FS but unlike the Fourier transform, which means that the signal cannot be exactly reconstructed from the NFM. This limits the use of the NFM but still permits the detection of nonstationary signal components. Nonstationary signal components, however, can be reconstructed directly from the results of the edge linking algorithm applied to the TFD.

There are many issues with comparing the performance of SDAs [31]. Differences in performance metrics and neonatal EEG databases make any comparisons difficult. Measures of performance such as epoch based sensitivity, epoch based specificity, event based seizure detection rate and event based false alarm rate are affected differently by changes in detection thresholds or post-processing stages and are also weighted by the ratio of seizure to nonseizure duration. Furthermore, depending on the definition, event based seizure detection rate and false alarm rates do not have a one-to-one relationship (Fig. 5). Differences in databases can affect results as traditional short duration recordings have lower artefact burden and more equal seizure to nonseizure duration ratios. This is due to the fact that attending neurophysiologists are, typically, called over during a period of intense seizure burden and are present for the entire recording. In the case of long duration recordings, such as used in this paper, the ratio seizure to nonseizure duration is strongly biased towards nonseizure and the artefact burden is relatively higher.

Nonetheless, the performance of the proposed SDA appears to exceed the first generation algorithms of [2,9,38–40,45], is comparable to the second generation algorithms of [3,36,41–43] but lags the third generation algorithm of [44]. The main advantage of the proposed SDA is the minimal use of information in decision making. The proposed SDA uses 96 discrete data points to represent 64 s of 8-channel EEG while the method of Temko et al. uses 3520 discrete data points, an order of magnitude difference.

The discriminatory performance of the test statistic η was reduced when the duration of the seizure was less than 64 s. The performance of η was also reduced from 0.944 to 0.902 when combined into a SDA and tested on the large database. This reduction was due, primarily, to the presence of artefact on the large neonatal EEG database. The artefacts that were most responsible for false alarms were repetitive artefacts such as those caused by respiration and heart rate and medium amplitude artefacts such as those caused by movement [14]. The repetitive artefacts resulted in significantly large values for η (although heart rate artefact was severely attenuated by the downsampling procedure) and medium amplitude artefacts resulted in significantly large values for aEEG. The presence of high frequency seizures in the database was of negligible influence on the SDA performance, as most high frequency seizures tended to degenerate into low frequency discharges.

The proposed SDA provides proof of concept of a newly derived decision statistic, estimated using the NFM, for the detection of seizure in neonatal EEG. It may be improved by incorporating additional features that represent the morphology of the seizure waveform, improvements in artefact detection, and using a more sophisticated classification system that is better able to segment the feature space. Additional improvements can be made by improving the implementation and efficiency of the NFM. While the application of advanced machine learning techniques offers great improvement to SDAs, there remains ample opportunity for the development and/or improvement of discriminatory, nonparametric neonatal EEG features.

5. Conclusion

The NFM is a new method of signal representation that can be used to detect pseudo-periodicity, such as seizure, in the neonatal EEG. The detection method uses a decision statistic defined as the power ratio between identified nonstationary signal components and the residual of the NFM. The NFM uses data-driven TF path integration to compress a TFD into a representation of nonstationary signal component power and mean frequency. The use of the NFM significantly improved the discriminative ability of the decision statistic by 9.4% in AUC compared to an estimate based on the FS even when the duration of the pseudo-periodicity was less than the duration of the analysis window. The incorporation of this decision statistic into a SDA based on two additional features of EEG amplitude resulted in detection performance that is comparable to existing second generation algorithms. Future work will introduce refinements to the method so as to improve the detection performance.

Acknowledgements

This work was supported in part by grants from Science Foundation Ireland (07/SRC/I1169, 08/RFP/CMS/1733 and 10/IN.1/B3036).

Conflict of interest

The authors would like to declare no conflicts of interest.

References

[1] Bracewell RN. The Fourier transform and its applications. 3rd ed. McGraw Hill; 2000.
[2] Gotman J, Flanagan D, Rosenblatt B. Automatic seizure detection in the newborn: methods and initial evaluation. Electroencephalography and Clinical Neurophysiology 1997;103:356–62.
[3] Greene BR, Marnane WP, Lightbody G, Reilly RB, Boylan GB. Classifier models and architectures for EEG-based neonatal seizure detection. Physiological Measurement 2008;29:1157–78.
[4] Thibeault-Eybalin MP, Lortie A, Carmant L. Neonatal seizures: do they damage the brain? Pediatric Neurology 2009;40:175–80.
[5] Björkman ST, Miller SM, Rose SE, Burke C, Colditz PB. Seizures are associated with brain injury in a neonatal model of hypoxia-ischemia. Neuroscience 2010;166:157–67.

[6] Miller SP, Weiss J, Barnwell A, Ferriero DM, Latal-Hajnal B, Ferrer-Rogers A, et al. Seizure-associated brain injury in term newborns with perinatal asphyxia. Neurology 2002;58:542–8.
[7] Lawrence R, Inder T. Neonatal status epilepticus. Seminars in Pediatric Neurology 2010;17:163–8.
[8] Celka P, Boashash B, Colditz P. Preprocessing and time-frequency analysis of newborn EEG seizures. IEEE Engineering in Medicine and Biology Magazine 2001;20:30–9.
[9] Celka P, Colditz P. A computer-aided detection of EEG seizures in infants: a singular spectrum approach and performance comparison. IEEE Transactions on Biomedical Engineering 2002;49:455–62.
[10] Boylan GB, Rennie J. Automated neonatal seizure detection. Clinical Neurophysiology 2006;117:1412–3.
[11] Clancy R, Legido A. The exact ictal and interictal duration of electroencephalographic neonatal seizures. Epilepsia 1987;28:537–41.
[12] Rankine L, Stevenson N, Mesbah M, Boashash B. A nonstationary model of newborn EEG. IEEE Transactions on Biomedical Engineering 2007;54:19–28.
[13] Stevenson NJ, Mesbah M, Boylan GB, Colditz PB, Boashash B. A nonlinear model of newborn EEG with nonstationary inputs. Annals of Biomedical Engineering 2010;38:3010–21.
[14] Mizrahi EM, Hrachovy RA, Kellaway P. Atlas of neonatal electroencephalography. 3rd ed Lippincott: Williams and Wilkins; 2004.
[15] Ristic B, Boashash B. Kernel design for time-frequency signal analysis using the Radon transform. IEEE Transactions on Signal Processing 1993;41:1996–2008.
[16] Baraniuk RG, Jones DL. Unitary equivalence: a new twist on signal processing. IEEE Transactions on Signal Processing 1995;43:2269–82.
[17] O'Toole JM, Boashash B. Time-frequency detection of slowly varying periodic signals with harmonics: methods and performance evaluation EURASIP Journal on Advances in Signal Processing 2011, doi:10.1155/2011/193797; 16 pages (Article ID 193797).
[18] Daković M, Thayaparan T, Stanković L. Time-frequency-based detection of fast manoeuvring targets. IET Signal Processing 2010;4:287–97.
[19] Baraniuk RG, Flandrin P, Janssen AJEM, Michel OJJ. Measuring time-frequency information content using Rényi entropies. IEEE Transactions on Information Theory 2001;47:1391–409.
[20] Toet MC, Hellstrom-Westas L, Groenendaal F, Eken P, de Vries LS. Amplitude integrated EEG 3 and 6 hours after birth in full term neonates with hypoxic-ischaemic encephalopathy. Archives of Disease in Childhood: Fetal and Neonatal Edition 1999;81:F19–23.
[21] Duda RO, Hart PE, Stork DG. Pattern classification. 2nd ed Wiley; 2001.
[22] Boashash B, editor. Time frequency signal analysis and processing: a comprehensive reference. Elsevier; 2003.
[23] Boashash B. Time-frequency signal analysis. In: Haykin S, editor. Advances in spectrum analysis and array processing, vol. 2. Prentice Hall; 1991.
[24] Bedrosian E. A product theorem for Hilbert transforms. Proceedings of the IEEE, 51. 1963. p. 686–9.
[25] Stevenson N, Rankine L, Mesbah M, Boashash B. Modelling newborn EEG background using a time-varying fractional Brownian process. In: Proceedings of the 15th European signal processing conference (EUSPICO). 2007. p. 1246–50.
[26] Peebles Jr PZ. Probability, random variables and random signal principles. 4th ed McGraw Hill; 2001.
[27] Rankine LJ, Mesbah M, Boashash B. IF estimation for multicomponent signals using image processing techniques in the time-frequency domain. Signal Processing 2007;87:1234–50.
[28] Larson RE, Hostetler RP, Edwards BH. Calculus. 5th ed D.C Heath and Co.; 1994.
[29] Farag A, Delp E. Edge linking by sequential search. Pattern Recognition 1995;28:611–33.
[30] Stevenson N, Mesbah M, Boashash B. Quadratic time-frequency distribution selection of seizure detection in the newborn. In: Proceedings of the 30th annual international conference of the IEEE engineering in medicine and biology society (IEEE-EMBC). 2008. p. 923–6.
[31] Temko A, Thomas E, Marnane WP, Lightbody G, Boylan GB. Performance assessment for EEG-based neonatal seizure detectors. Clinical Neurophysiology 2011;122:474–82.
[32] Zoubir AM, Boashash B. The bootstrap and its application in signal processing. IEEE Signal Processing Magazine 1998;15:56–76.
[33] Flandrin P. A time-frequency formulation of optimal detection. IEEE Transactions on Acoustics, Speech and Signal Processing 1988;36:1377–84.
[34] Greene BR, Faul S, Marnane WP, Lightbody G, Korotchikova I, Boylan GB. A comparison of quantitative EEG features for neonatal seizure detection. Clinical Neurophysiology 2008;119:1248–61.
[35] Box GEP, Jenkins GM, Reinsel GC. Time series analysis, forecasting and control. 3rd ed Prentice Hall; 1994.
[36] Navakatikyan MA, Colditz PB, Burke CJ, Inder TE, Richmond J, Williams CE. Seizure detection algorithm for neonates based on wave-sequence analysis. Clinical Neurophysiology 2006;117:1190–203.
[37] Deburchgraeve W, Cherian PJ, De Vos M, Swarte RM, Blok JH, Visser GH, et al. Automated neonatal seizure detection mimicking a human observer reading EEG. Clinical Neurophysiology 2008;119:2447–54.
[38] Liu A, Hahn JS, Heldt GP, Coen RW. Detection on neonatal seizures through computerized EEG analysis. Electroencephalography and Clinical Neurophysiology 1992;82:30–7.
[39] Roessgen M, Zoubir AM, Boashash B. Seizure detection of newborn EEG using a model-based approach. IEEE Transactions on Biomedical Engineering 1998;45:673–85.
[40] Smit LS, Vermeulen RJ, Fetter WPF, Strijers RLM, Stam CJ. Neonatal seizure monitoring using non-linear EEG analysis. Neuropediatrics 2004;35:329–35.
[41] Mitra J, Glover JR, Ktonas PY, Kumar AT, Mukherjee A, Karayiannis NB, et al. A multistage system for the automated detection of epileptic seizures in neonatal encephalography. Journal of Clinical Neurophysiology 2009;26:218–26.
[42] Aarabi A, Grebe R, Wallois F. A multistage knowledge-based system for EEG seizure detection in newborn infants. Clinical Neurophysiology 2007;118:2781–97.
[43] Cherian PJ, Deburchgraeve W, Swarte RM, De Vos M, Govaert P, Van Huffel S, et al. Validation of a new automated neonatal seizure detection system: a clinician's perspective 2011, doi:10.1016/j.clinph.2001.01.043.
[44] Temko A, Thomas E, Marnane WP, Lightbody G, Boylan GB. EEG-based neonatal seizure detection with support vector machines. Clinical Neurophysiology 2011;122:464–73.
[45] Faul S, Boylan G, Connolly S, Marnane L, Lightbody G. An evaluation of automated neonatal seizure detection methods. Clinical Neurophysiology 2005;116:1533–41.